Molecular Cell, Vol. 8, 569–580, September, 2001, Copyright ©2001 by Cell Press

Differential Dimer Activities of the Transcription Factor Oct-1 by DNA-Induced Interface Swapping

Attila Reményi,[1,5] Alexey Tomilin,[2,5] Ehmke Pohl,[1] Katharina Lins,[2] Ansgar Philippsen,[3] Rolland Reinbold,[2] Hans R. Schöler,[2,4] and Matthias Wilmanns[1,4]

[1] European Molecular Biology Laboratory
Hamburg Outstation
c/o DESY
Notkestrasse 85
D-22603 Hamburg
Germany

[2] Center for Animal Transgenesis
and Germ Cells Research
New Bolton Center
School of Veterinary Medicine
Department of Animal Biology
University of Pennsylvania
382 West Street Road
Kennett Square, Pennsylvania 19348

[3] Biozentrum Basel
University of Basel
Klingelbergstrasse 70
CH-4056 Basel
Switzerland

Summary

Two crystal structures of Oct-1 POU domain bound to DNA provide a rationale for differential, conformation-dependent recruitment of transcription cofactors. The POU-homeo and POU-specific subdomains of Oct-1 contain two different nonoverlapping pairs of surface patches that are capable of forming unrelated protein-protein interfaces. Members of the POU factor family contain one or two conserved sequence motifs in the interface that are known to be phosphorylated, as noted for Oct-1 and Pit-1. Modeling of Oct-4 reveals the unique case where the same conserved sequence is located in both interfaces. Our studies provide the basis for two distinct dimeric POU factor arrangements that are dictated by the architecture of each DNA response element. We suggest interface swapping in dimers could be a general mechanism of modulating the activity of transcription factors.

Introduction

Members of the POU transcription factor family are involved in a broad range of biological processes ranging from housekeeping gene functions (Oct-1) to programming of embryonic stem cells (Oct-4) and the development of immune responses (Oct-1, Oct-2) (Schöler, 1991; Ryan and Rosenfeld, 1997). However, according to the latest global sequencing reports, human, fly, and worm genomes encode only fifteen, five, and four POU factors, respectively (Venter et al., 2001). Therefore, members of this transcription factor family need to rely on multilevel control mechanisms such as posttranslational modification, interaction with heterologous transcription regulators, and flexible DNA binding to perform these multiple tasks. A linker joining the POU-specific (POU_S) and the POU-homeo domain (POU_H) confers the flexibility inherent to members of the POU factor family. This linker is variable both in sequence and length (15–56 residues). Since both domains are structurally and functionally autonomous in DNA binding, various arrangements on DNA are possible (Herr and Cleary, 1995).

POU factors were originally identified to function as monomeric transcription regulators, for instance, when they bind to the DNA octamer motif (Staudt et al., 1986; Schöler et al., 1989). However, more recently, their capability to homo- and heterodimerize on specific DNA response motifs has received substantial attention (Jacobson et al., 1997; Botquin et al., 1998; Rhee et al., 1998; Scully et al., 2000; Tomilin et al., 2000). The Palindromic Oct factor Recognition Element (PORE), ATTT GAAATGCAAAT, within the first intron of the *osteopontin* (*OPN*) gene, was initially identified as an Oct-4 DNA responsive element. It mediates strong transcriptional activation in preimplantation mouse embryos and cell lines derived thereof (Botquin et al., 1998). Oct-4 binds to the PORE in a monomer/dimer equilibrium, in which single nucleotide replacements are sufficient to enhance or diminish dimerization. In vitro, the PORE behaves as a general Oct factor recognition element (Botquin et al., 1998). To further investigate the general dimerization potential of Oct factors, sequences related to the *Prl* Pit-1 response element (Jacobson et al., 1996) were characterized. These so-called MORE sequences (More palindromic Oct factor Recognition Elements) are found in various promoters (Tomilin et al., 2000). All members of the Oct family tested bind cooperatively as homo and heterodimers to the consensus MORE (Tomilin et al., 2000).

The transcriptional activity of Oct-1 on the octamer motif in B cells is regulated by the lymphoid-specific coactivator OBF-1 (OCA-B, BOB-1) that clamps the POU_H and POU_S subdomains together and thus enhances their DNA binding affinity (Sauter and Matthias, 1998; Chasman et al., 1999). However, the Oct-1 dimer formed on MOREs within immunoglobulin heavy chain promoters (V_H) fails to interact with OBF-1. In contrast, the Oct-1/PORE dimeric complex can interact and synergize in transcriptional activation with this cofactor. These findings established the paradigm of differential transcriptional regulation mediated by two distinct POU dimer configurations (Tomilin et al., 2000).

To elucidate the structural basis of this phenomenon, we have solved two crystal structures of the Oct-1 POU domain bound to the MORE and PORE. By direct comparison, these structures demonstrate how the same polypeptide chain can form two different dimer arrangements with two distinct protein-protein interfaces. These data introduce the concept of distinct transcription fac-

[4] Correspondence: wilmanns@embl-hamburg.de (M.W.), scholer@vet.upenn.edu (H.S.)

[5] These authors contributed equally to this work.

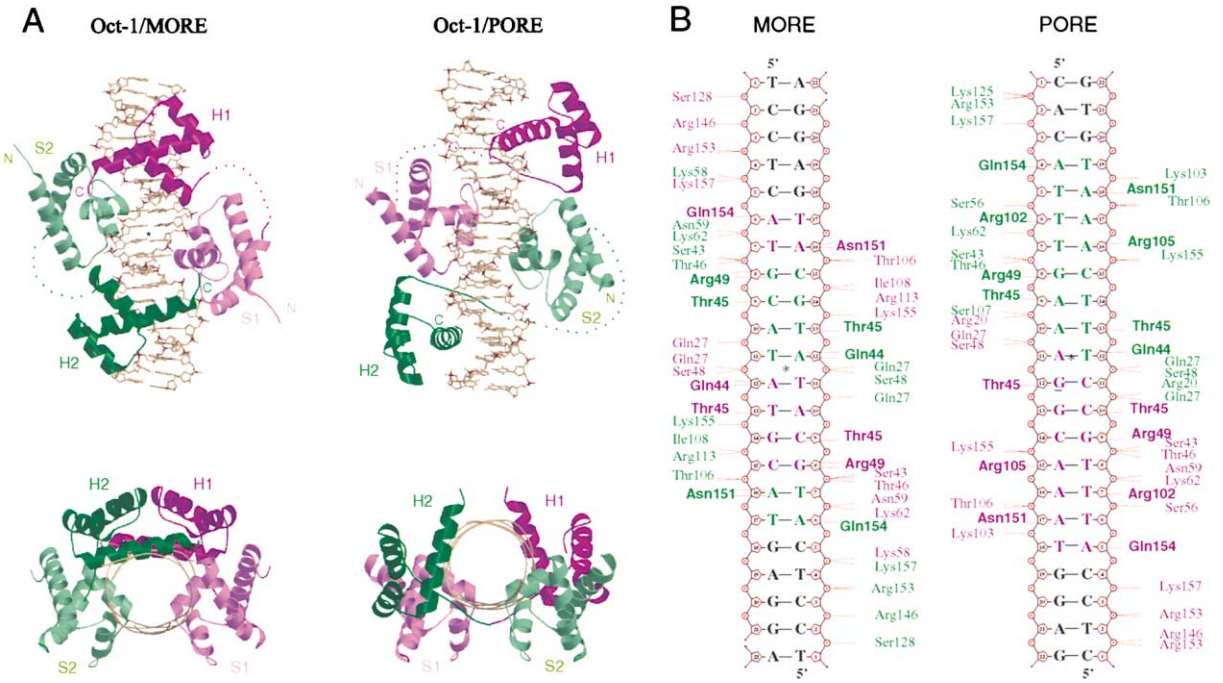

Figure 1. Different Domain Arrangements in the Oct-1/MORE and Oct-1/PORE Complexes Mediated by Conserved Protein-DNA Interactions

(A) The bipartite Oct-1 POU domain binds to both DNA responsive elements as a homodimer. In both structures, each POU-specific domain (POU_S, S) is folded as a four-helix bundle, and each POU-homeo domain (POU_H, H) is comprised of three α helices. Each protein molecule is depicted in the same color with different amounts of saturation for the two subdomains (POU_S, less saturated; POU_H, more saturated). In the Oct-1/PORE complex, the protein molecule bound to the octamer-like half-site of the PORE element (5′-AGGCAAAT) is colored in magenta, and the molecule bound to the nonoctamer-like half-site (5′-TTTCAAAT) is in green. This coloring scheme is maintained in all subsequent figures. The lower panel shows the two structures viewed along the DNA axis. The asterisk indicates the palindromic center of the MORE oligonucleotide, which coincides with a crystallographic 2-fold axis. "N" and "C" designate the N terminus and the C terminus of each POU molecule, respectively. The approximate locations of the linkers, which are invisible in the structural model due to their flexibility, are shown as dotted lines.

(B) NUCPLOT representation (Luscombe et al., 1997) showing the hydrogen bond (H bond) interactions between POU molecules and the MORE and PORE DNA elements. The DNA phosphate backbone-mediated H bond interactions are depicted in regular font; the DNA sequence-specific interactions are in bold. The asterisks mark the palindromic and the semipalindromic centers of the MORE and PORE motifs, respectively. For simplicity, water-mediated protein-DNA interactions have not been included.

tor dimerization that depends on the sequence and the spacing of the protein domain binding motifs of the DNA response element. Thus, it extends previous models of protein-DNA complex formation mediated by ligand-induced allosteric effects (Lefstin and Yamamoto, 1998). The members of the nonsteroid nuclear receptor family, for example, provide another mode of transcription factor dimerization dictated by the binding site, the hormone response element (HRE). HREs consist of two core hexad sequences, AGGTCA. These could form direct, inverted, or everted repeats. On inverted and everted repeats, the receptors dimerize only via a specific surface patch within the carboxy-terminal ligand binding domain. On direct repeats, however, the receptors form an additional interface between the conserved zinc finger DNA binding domains (Mangelsdorf and Evans, 1995). The DNA sequence-mediated dimerization of POU proteins is different since the distinct surface patches involved in dimer interface formation are both located on the DNA binding POU domain. Our results show how swapping protein-protein interfaces between different quaternary arrangements of POU factor/DNA complexes can regulate transcriptional activity.

Results

Overall Structures of the Oct-1/DNA Complexes

We have solved the crystal structures of the DNA binding segment of Oct-1 in complex with the MORE or PORE at a resolution of 1.9 Å and 2.7 Å, respectively (Figure 1, more details in Experimental Procedures). Since the Oct-1 binding segment of the MORE is palindromic (ATGCATATGCAT), it was not surprising that only one-half of the protein-DNA dimer was found in the asymmetric unit of the Oct-1/MORE crystals. The complete dimer complex is defined by a crystallographic 2-fold axis across the palindromic center of the MORE. The Oct-1/PORE structure contains the complete Oct-1 homodimer bound to the PORE DNA (ATTTGAAAGGCAAAT). This semipalindromic element, based solely on sequence similarity to the consensus octamer motif (ATG CAAAT), can be divided into an octamer-like (AGG CAAAT) and into a nonoctamer-like (TTTCAAAT) half-site (Figure 1B).

In the MORE complex, dimer binding extends over 12 base pairs, while a more extended segment of 15 base pairs of the PORE is bound by the Oct-1 dimer, leading

to a less compact protein-DNA arrangement. As in previously described structures of POU/DNA complexes, the linker region of Oct-1, connecting the POU_S and POU_H domains, remained invisible in the final electron density for both complexes. Therefore, the four domains (two POU_S and two POU_H) that compose the protein homodimer appear to be bound to DNA in a heterotetrameric arrangement (Figure 1A).

Structurally Conserved Protein Domain-DNA Interactions

The Oct-1 POU factor binds to DNA in a bipartite fashion. The binding topography is the same in both complexes in the sense that the POU_S domains are situated proximal to the center of each DNA element, while the POU_H domains bind at distal positions (Figure 1B). In the MORE complex, the DNA binding sites for POU_H and POU_S overlap by 2 base pairs within each MORE half-site, whereas in the PORE complex, the two POU_S domains share 1 base pair in the center of the PORE motif (Figure 1B). Due to the nonpalindromic nature of the PORE, the two POU_S domains bind to nonidentical sites, AGGC and TTTC.

Each POU_H domain is bound to a distal AT-motif. On the MORE, this motif is located at positions 1-2 and 11-12, while on the PORE it is located at positions 1-2 and 14-15. In both complexes, the C-terminal helix 3 of each POU_H domain is situated in the major groove, with base-specific interactions of the side chains of Asn151 and Gln154. In the PORE complex, the arginine residues of the N-terminal part of POU_H (Arg102 and Arg105) form DNA sequence-specific hydrogen bonds (H bonds) with the base pairs in positions 3-4 and 12-13. These interactions are formed via the minor groove within each half-site of the PORE motif (Figure 1B). They are not visible in the Oct-1/MORE complex because this part is disordered. The POU_S domains interact with bases in the major groove via their third α helix. In the two complexes, the side chains of residues Gln44, Thr45, and Arg49 almost identically contribute with base-specific interactions to each POU_S binding site (Figure 1B).

Nonoverlapping Protein-Protein Interfaces

The two structures of the Oct-1 POU factor in complex with the MORE and PORE demonstrate how the same transcription factor can form unrelated arrangements using different, nonoverlapping surface patches for domain-domain association. Each arrangement is induced by the specific positions and nature of the four protein binding segments on the respective DNA element. The heterotetrameric arrangement of the POU dimers allows two alternatives for POU_S-POU_H interface formation, one across the center of each DNA response motif (vertical in Figure 2) and one within one half-site (horizontal in Figure 2). However, the crystal structures demonstrate that each complex reveals only one type of interface, either across the DNA center or within each DNA half-site.

MORE-Induced POU_S-POU_H Interface

In the Oct-1/MORE structure, there are two identical protein-protein contacts forming between a POU_S and a POU_H domain within each half-site of the palindromic MORE motif (Figure 2A). The buried surface per domain is about 550 Å^2 (determined after Lee and Richards, 1971). A central feature of this interface is the docking of the C-terminal residues 157–160 of the POU_H domain onto the loop region between helix 3 and 4 of the POU_S domain. The side chain of Ile159 fits into a hydrophobic cavity of the POU_S subdomain, which forms a "knob-in-the-hole" structure (Figure 2C). Furthermore, additional interactions are mediated by several H bonds, mostly from main chain atoms except for one side chain contribution by Asn160. This interface is reminiscent of those found in the Pit-1/DNA complexes (Jacobson et al., 1997; Scully et al., 2000).

PORE-Induced POU_S-POU_H Interface

The two main interfaces formed in the Oct-1/PORE complex are located across the center of the PORE motif, as opposed to the interface observed in the Oct-1/MORE structure. These interfaces are not identical, reflected in the different amounts of buried surface areas of 220 Å^2 and 500 Å^2, hence termed IF1 and IF2, respectively (Figure 2B). Central to this interface is the N terminus of the POU_H domain, which interacts with the minor groove of the PORE-DNA as well as with residues of a POU_S domain (Figure 2D). In the larger interface (IF2), one phosphate group within the minor groove (position 10 of the PORE) forms H bonds with Arg20 from the POU_S and Ser107 from the POU_H domain (Figures 1B and 2D). This DNA-mediated POU_S-POU_H contact is surrounded by two POU_S-POU_H salt bridges, Asp29-Lys104 and Lys22-Glu109. Like the knob-in-the-hole interaction by Ile159 in the Oct-1/MORE complex, the exposed Ile21 from the POU_S domain penetrates into a hydrophobic surface patch of the POU_H domain (Figure 2D).

Within the smaller interface (IF1), the only specific interaction is the POU_S-POU_H salt bridge between Asp29 and Lys104. Ser107 is more exposed to the solvent than in the IF2 interface. Thus, the phosphate group from the minor groove forms only one H bond with Arg20 (Figure 1B). The observed asymmetry in the PORE interface (IF1 and IF2) can be explained by the different minor groove parameters at the two half-sites of the semipalindromic PORE, as calculated using the program CURVES (Lavery and Sklenar, 1988). Only the minor groove at the nonoctamer half-site, which is about 10% narrower and deeper than that of the octamer half-site, allows a tight fit of the two interacting POU domains within the IF2 interface (Figure 2D).

DNA-Induced POU_S-POU_H Interfaces Are Nonoverlapping

To further validate our structural data on MORE- and PORE-mediated dimer formation, we mutated residues in Oct-1 that are involved in specific interactions within the two domain/domain interfaces, as inferred from the two crystal structures. Since the residues that contribute to the MORE-type interface do not overlap with those within the PORE dimer, we were able to design mutant versions of the protein that selectively form one complex but not the other (Figure 2E). To confirm correct folding and canonical DNA binding activity, each mutant was tested for its ability to bind as a monomer to the consensus octamer site within the promoter region of the immunoglobulin κ gene. As expected, the mutant, which was designed to interfere with the MORE domain-domain interface (I159D, N160A; see Figure 2C), dimerized on the PORE but not on the MORE. Conversely, the PORE-

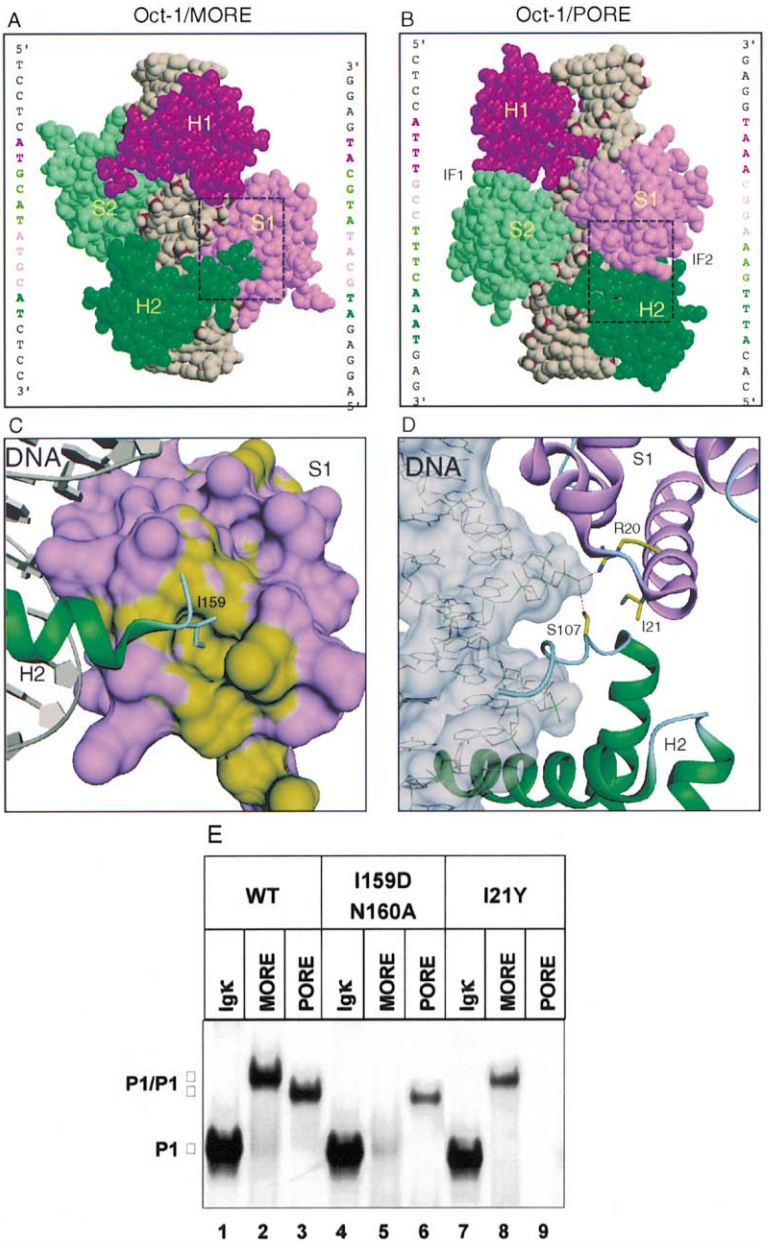

Figure 2. Two Distinct POU_S-POU_H Interfaces in the Oct-1/MORE and Oct-1/PORE Complexes

(A and B) The different domain arrangements adopted in the two complex structures are formed by distinct domain-domain contacts. The color code of each DNA, which is shown vertically to left and right of each complex, reflects its specific interaction with the corresponding Oct-1 domains. The Oct-1/PORE complex is rotated 180° along the DNA axis with respect to Figure 1 to show the DNA from its protein-covered side.

(C) Close-up of the POU_{S1}-POU_{H2} interface of the Oct-1/MORE complex (S1-H2), emphasizing the hydrophobic interactions of Ile159 from the C-terminal part of the POU_H domain with POU_S. The C-terminal helix of the POU_H is depicted in green; the POU_S is shown as a surface representation in magenta with the hydrophobic residues in yellow.

(D) Close-up of the POU_{S1}-POU_{H2} interface of the Oct-1/PORE complex focusing on the interplay between protein-DNA and protein-protein interactions (S1-H2). The N-terminal nonhelical segment of the POU_H is situated in the minor groove of the PORE element. One DNA phosphate group forms H bonds with Arg20 (POU_S) and Ser107 (POU_H). The figure depicts the larger interface (IF2; see text). POU_S is colored in magenta; POU_H in green. The DNA molecule is shown as a surface representation in gray.

(E) Interface mutants selectively disrupt the MORE- and PORE-type Oct-1 dimer. Amino acid residues from the MORE- or PORE-type POU_S-POU_H interfaces were mutated to disrupt the respective dimer (MORE-interface mutant: I159D, N160A; PORE-interface mutant: I21Y). According to the EMSA, the interface-specific mutations do not interfere with monomer binding to the Igκ octamer site but selectively disrupt the MORE- or PORE-type complex formation. WT, wild-type POU domain of Oct-1; Igκ, oligonucleotide containing the octamer motif from the immunoglobulin kappa chain promoter; P1, POU monomer/DNA complex; and P1/P1, POU dimer/DNA complex. Notice that the Oct-1 dimer complexes with MORE and PORE migrate differently.

interface mutant (I21Y; see Figure 2D) did not dimerize on the PORE but did so on the MORE (Figure 2E). These results demonstrate that the PORE- and MORE-specific POU_S-POU_H interfaces not only appear to be structurally independent but are also functionally modular and autonomous.

Connectivity of POU_S and POU_H Domains by an Unstructured Linker

The invisibility of the linker connecting POU_S and POU_H in each polypeptide chain impairs unambiguous structural assignment of intramolecular domain-domain connectivity in the Oct-1/MORE and Oct-1/PORE crystal structures, similarly to previously solved POU/DNA structures (Klemm et al., 1994; Jacobson et al., 1997; Scully et al., 2000). The consistently observed unstructured nature of this segment suggests that flexibility of the linker could be an inherent property of POU factors (Herr and Cleary, 1995; Phillips and Luisi, 2000). However, linker connectivity needs to be addressed when considering possible binding cooperativity in POU dimer/DNA interaction. Below, we will combine topography considerations with biochemical data to provide evidence for the POU_S-POU_H connectivity in the Oct-1/MORE and Oct-1/PORE complexes.

There is no ambiguity about the POU_S-POU_H connectivity in the Oct-1/octamer motif monomeric crystal structure (Klemm et al., 1994). This arrangement is equivalent to one half of the dimeric Oct-1/PORE complex, suggesting a duplicated octamer-motif-like arrangement in which each polypeptide chain is bound to one half-site of the PORE. This model postulates that the POU_H-POU_S protein interfaces in the PORE (IF1 and IF2; see Figure 2) are formed between the two protein

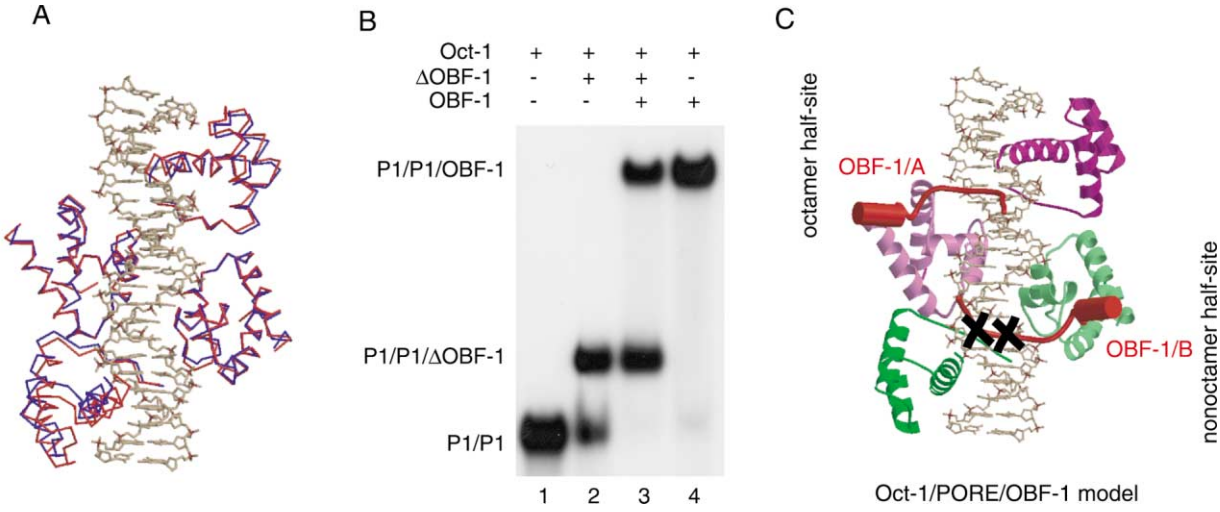

Figure 3. Model of Oct-1/PORE/OBF-1 Ternary Complex

(A) Superposition of the Oct-1 POU domain from the Oct-1/octamer/OBF-1 peptide ternary complex (Chasman et al., 1999) with the two POU domain monomers from the Oct-1/PORE crystal structure (see text). The POU domain from the ternary complex is shown as a Cα-trace in red, the Oct-1/PORE complex in blue. Notice that the POU_H domain superimposes well only for the monomer bound to the upper (octamer-like) half of the PORE motif. The other POU_H shows an offset and is moved away from the DNA.

(B) EMSA results with the PORE oligonucleotide, the POU domain of Oct-1, full-length OBF-1 protein, and a 44 amino acid containing OBF-1 peptide (ΔOBF-1). The binding of the full-length coactivator (~30 kDa) and the OBF-1 peptide (~5 kDa) to the Oct-1/PORE dimeric complex (P1/P1) both result in the formation of differently migrating ternary complexes. The absence of a complex with intermediate mobility—between these two ternary complexes—indicates that the Oct-1/PORE dimer can bind to only one OBF-1 molecule at a time (see lane 3).

(C) The Oct-1/PORE complex could contain two coactivator binding sites at first glance. The figure shows the Oct-1/PORE crystal structure with the superimposed coactivator peptides in red. Due to the different geometric parameters of the PORE DNA half-sites, the lower site is not capable of binding to OBF-1 (crossed, see text).

molecules and thus contribute to dimer stability. According to this model, the correct spacing and relative orientation of the two sets of POU_S/POU_H binding sites are critical for protein-protein interactions across the half-sites of the PORE. This has been confirmed by previous data on the related Oct-4/PORE complex, demonstrating that the correct spacing of the half-sites is an absolute requirement for Oct factor dimer formation (Botquin et al., 1998).

The Oct-1/MORE complex, in contrast, is reminiscent of the structure of the related Pit-1 POU factor with the synthetic *Prl*-like DNA sequence (Jacobson et al., 1997). Distance considerations and mutation data on this complex indicated an unambiguous preference for a dimer model in which POU_S-POU_H dimer contacts form within each half-site of the DNA (Jacobson et al., 1997). Consequently, the spacing of the two half-sites should not have a direct influence on the POU_S-POU_H dimer interface but should only be restricted by the length of the POU_S-POU_H linker. This hypothesis has recently been confirmed by a Pit-1 complex structure with the *GH* DNA response element, in which the spacing of the half-sites was increased by 2 base pairs (Scully et al., 2000). Furthermore, in an analogous experiment, we have shown that the spacing between the two POU_S/POU_H binding sites of the MORE can be extended by up to 2 base pairs without abolishing Oct-1 dimer formation (Tomilin et al., 2000).

Structural Basis of OBF-1 Interaction with the Oct-1/PORE Complex

The B cell lineage-specific coactivator OBF-1 complements the transcriptional activity of Oct-1 on the octamer consensus element (Sauter and Matthias, 1998). A crystal structure with a 44 residue fragment of OBF-1 bound to the Oct-1/octamer motif complex revealed that this segment of OBF-1 simultaneously binds the DNA and both the POU_S and POU_H domains of the Oct-1 monomer, thereby forming a clamp-like contact between them through the major groove (Chasman et al., 1999). Recently, we have demonstrated that OBF-1 specifically fails to interact with the MORE-type configuration but is capable of binding to the PORE-type configuration of Oct-1 (Tomilin et al., 2000), implying that structural differences between the two dimers lead to differential recruitment of this coactivator.

The crystal structure of the Oct-1/PORE dimer complex suggests the way OBF-1 could bind to the PORE-mediated Oct-1 dimer. This structure shows how the deviations of the PORE sequence from palindromic symmetry lead to differences in the geometric parameters of the two DNA half-sites which in turn result in an asymmetric dimer arrangement. Superposition of the two half-site POU_S-POU_H arrangements of the PORE dimer onto the Oct-1/octamer/OBF-1 complex (Chasman et al., 1999) shows that only one of them, covering the octamer-like half-site of the PORE (ATTTGAAAGG CAAAT), matches the OBF-1 binding site geometry of the Oct-1/octamer/OBF-1 complex (Figure 3A). Within the other POU_S/POU_H/DNA associate from the nonoctamer half-site, the POU_H domain is displaced by about 3 Å with respect to the arrangement of the Oct-1/octamer motif complex as a reference. In this conformation, the C terminus of the third POU_H helix, which is critical for POU/OBF-1/DNA complex formation (Chasman et al., 1999), would be too far away to be involved in any spe-

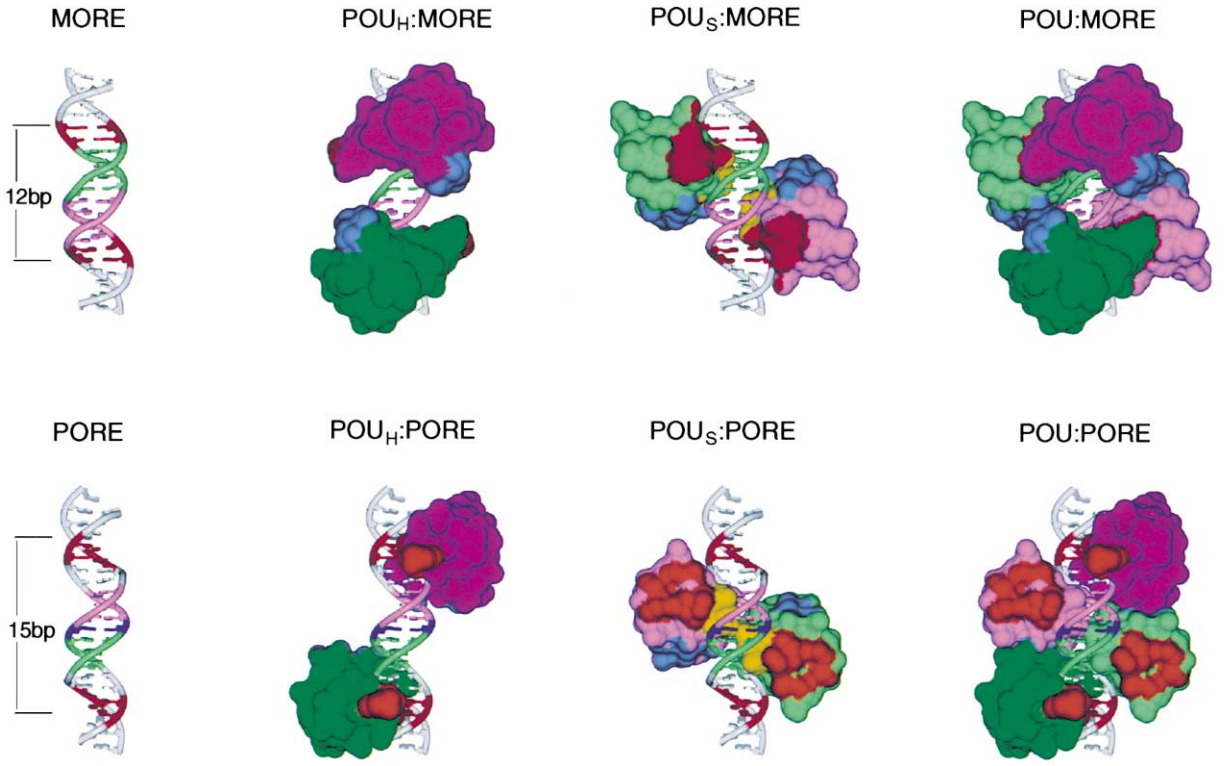

Figure 4. Different DNA Subsite Spacing of MORE and PORE Induces Different Quaternary Structure Formation by Alternative Domain/Domain Surface Patches

Left to right: structure of the MORE and PORE DNA, the different subdomain/DNA complexes (POU$_H$, POU$_S$) from the Oct-1/MORE and the Oct-1/PORE crystal structures, and the complete dimeric complexes. The POU$_H$ binding AT subsite is colored in red to indicate the boundaries in each binding site; the POU$_S$ binding boxes (ATGC, AGGC, or TTTC) are indicated in the color of the POU$_S$ that bind them. The shared base pair between the two POU$_S$ binding subsites of the PORE is colored blue. The conserved protein domain-DNA surface patches of the POU$_S$ and the POU$_H$ domains are colored in yellow and red, respectively. (This patch, however, for the POU$_H$ domain is not visible from these orientations—it is seen only in part on the upper domain of the POU$_H$:PORE subcomplex). The MORE- and the PORE-type dimerization surface patches are marked in brick red and gray-blue, respectively. Notice the nonoverlapping nature of the two interfaces.

cific interactions with the coactivator. The structural data are further validated in a biochemical experiment showing that only one OBF-1 coactivator molecule binds to the Oct-1 PORE dimer (Figure 3B). In essence, these data demonstrate that regulation of Oct-1 by binding of the coactivator OBF-1 not only depends on its overall dimer arrangement but also on the specific geometry of the DNA element (Figure 3C).

Discussion

Comparison of the two structures of the POU transcription factor Oct-1 reveals how a member of this family can rearrange its quaternary structure in the presence of specific DNA response motifs. The two arrangements are possible because each of the two subdomains, POU$_S$ and POU$_H$, contains two binding sites both suitable for forming a POU$_S$-POU$_H$ domain-domain interface. There is evidence for at least one of the two pairs of binding sites to be employed in the recruitment of the Oct-1 coactivator OBF-1 while not being involved in POU$_S$-POU$_H$ interface formation. By the presence of this 2-fold arsenal of surface patches per subdomain, members of the POU transcription factor family have evolved a unique mechanism for structural plasticity. This mechanism could be employed to compensate for the lack of flexibility at the secondary and tertiary structural level within each of their small, compact subdomains (POU$_S$ and POU$_H$).

DNA-Induced Interface Swapping

Critical to the formation of alternative Oct-1 dimers with the MORE or PORE motifs is the capability of the POU domain to utilize two different, nonoverlapping protein surface patches to form POU$_S$-POU$_H$ interfaces. Although an isoleucine residue plays a prominent role on both interfaces (I21 from the POUs domain in the PORE interface; I159 from the POU$_H$ domain in the MORE interface), we were not able to detect any other significant similarity between them either in sequence or in structure. Specific mutants that abolish the capability of Oct-1 to form alternative dimer arrangements, resulting in either MORE-only or PORE-only dimers, further support the independence of both POU$_S$-POU$_H$ interfaces.

In Figure 4, we illustrate schematically why binding of Oct-1 to the MORE and PORE motifs results in different protein arrangements. Since the POU$_S$-POU$_H$ interface is across the center of the DNA in the PORE complex, correct spacing and orientation of the two polypeptide chains, defined by the POU$_S$ and POU$_H$ binding sites of

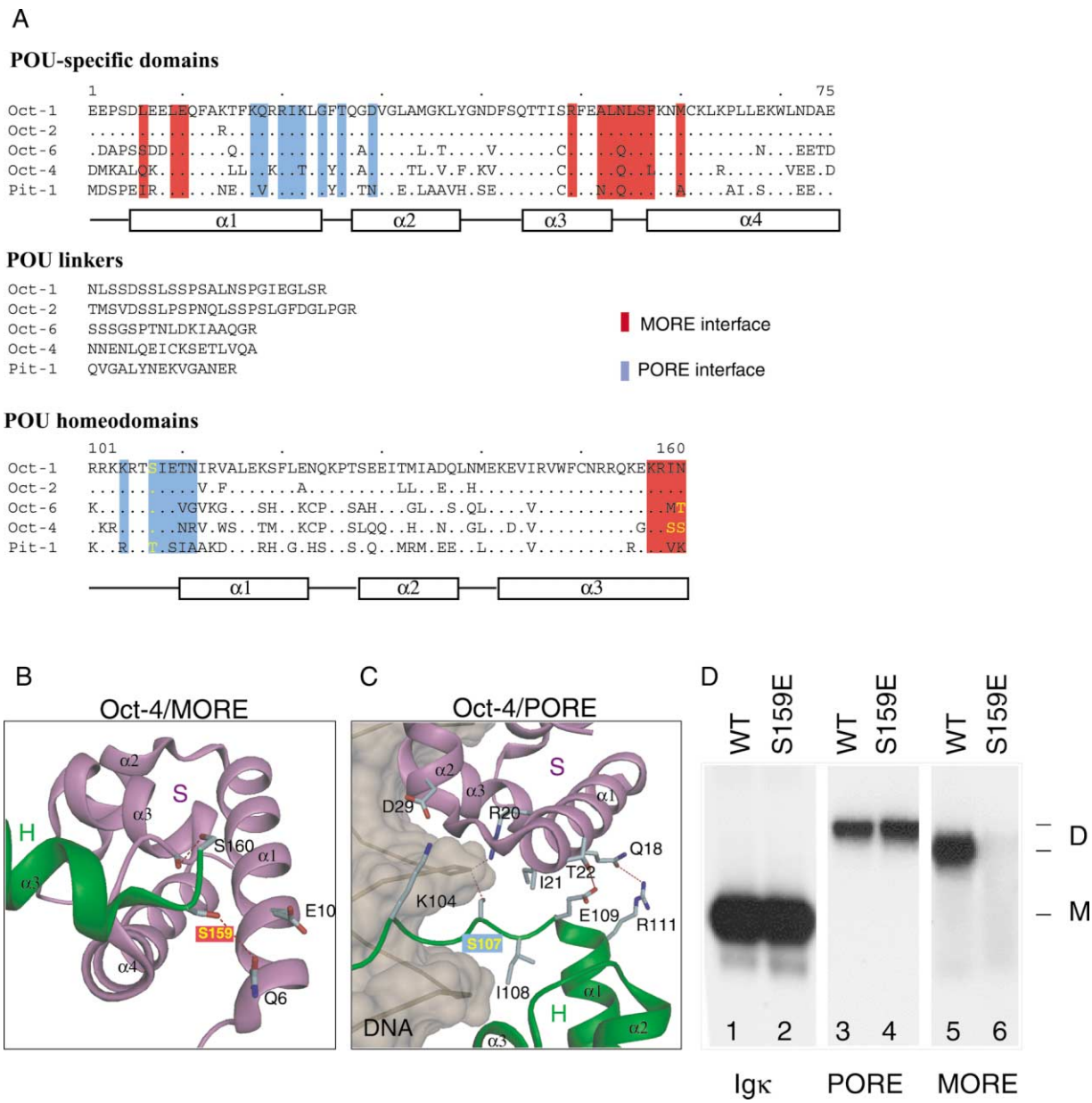

Figure 5. The MORE- and PORE-Type Interfaces Are Structurally Conserved in the POU Transcription Factor Family

(A) Sequence alignment of POU domains from different transcription factors reported to dimerize in a DNA sequence-dependent fashion. Amino acid residues conserved to Oct-1 are indicated by dots. Residues involved in POU_S-POU_H interface formation in the Oct-1/MORE and Oct-1/PORE crystal structures are highlighted red and blue, respectively. Serine and threonine residues that are candidates for posttranslational modification are marked in yellow.

(B and C) Oct-4/MORE and Oct-4/PORE homology model built with WHAT IF (Vriend, 1990) using the coordinate file of the respective crystal structures with Oct-1. Due to sequence variation in the two interfaces, both models predict new side chain-specific H bond formations between the two POU molecules. This finding demonstrates the versatile nature of the MORE- and the PORE-type interface. Ser159 and Ser107 play a central role in the MORE- and PORE-like interaction, respectively.

(D) EMSA using an Oct-4 mutant containing a phosphorylation imitating mutation in the MORE dimerization interface (S159E). The Ser159Glu mutation selectively disrupts dimerization only on the MORE but not on the PORE motif. WT, wild-type Oct-4 protein; Igκ, oligonucleotide containing the octamer motif from the immunoglobulin kappa chain promoter; M, monomer; and D, dimer.

the DNA, are strictly required for correct dimer formation. Any other spacing would either lead to steric domain clashes or to the loss of the interface. However, binding to shorter DNA elements by Oct-1 is indeed feasible by changing POU_S-POU_H interfaces from an "across two half-sites" PORE-type to a "within one half-site" MORE-type interaction. This is possible only because the POU_S and POU_H domains bear redundant, functionally identical protein-protein surface patches to form nonoverlapping POU_S-POU_H interfaces. A change in the spacing of protein binding sites on the DNA by 1 base pair transforms into a rotational component of

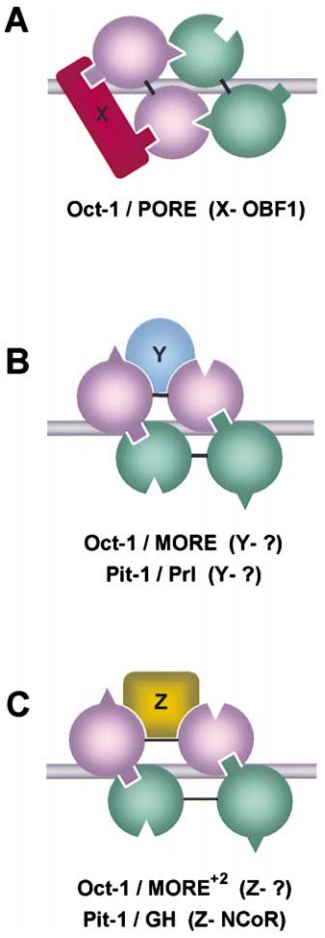

Figure 6. Model for Selective Recruitment of Cofactors by POU Dimers

Schematic representation of POU dimer arrangements bound to (A) the PORE; (B) the MORE (Oct-1) or Prl (Pit-1); and (C) the MORE^{+2} (Oct-1) or GH (Pit-1) DNA response elements, which contain a 2 base pair insertion between the two half-sites when compared to MORE/Prl. The different quaternary arrangements of POU subdomains (indicated by spheres) either expose or bury the MORE- or the PORE-type dimerization interfaces. The MORE-type interface is indicated as rectangular indentations (on the surface of POU_S) and protrusions (on the surface of POU_H). The PORE-type interface is indicated by triangles. The open MORE-type interface is used for binding of OBF-1 in the Oct-1/PORE dimer. On the other hand, the PORE-type interface could be potentially engaged for specific cofactor recruitment ("Y" and "Z"), which could either be selective with respect to the type of dimer configuration (MORE versus PORE) or to the spacing of half-sites within one configuration. The second type of selectivity is only applicable for the MORE configuration, because the PORE configuration does not allow different spacing of DNA half-sites. The N-CoR corepressor complex (Scully et al., 2000) selectively binds to Pit-1 in complex with GH ("Z") but not with Prl ("Y").

about 36° and a translation of ~3.6 Å along the DNA axis. Therefore, different spacing arrangements of the POU subdomain binding sites yield different quaternary POU dimer/DNA structures. Figure 4 illustrates how the POU_S and POU_H surface patches, forming the POU_S-POU_H interface in one complex, become exposed in the alternative complex.

Structural and biochemical data suggest that the observed interface swapping leads to domain swapping (Klemm et al., 1994; Botquin et al., 1998; Scully et al., 2000; Tomilin et al., 2000), although an opposite model for the PORE complex cannot be formally ruled out. In reference to the two POU_H domains, the PORE/MORE swapping would result in flipping of each of the two POU_S domains from one DNA half-site to the opposite and vice versa.

Interface Swapping as a Common Property of POU Factors

Despite their different functions in vivo, POU factors display considerable sequence similarity, most particularly within the segments that are involved in DNA binding and dimer formation (Figure 5A). Earlier studies of the MORE and PORE *cis* regulatory elements revealed that both motifs mediate versatile homo and heterodimerization among the four Oct factors (Oct-1, Oct-2, Oct-4, and Oct-6) tested (Botquin et al., 1998; Tomilin et al., 2000). Computer models generated for all these homo and heterodimers indicate that they can be formed without steric clashes and by preserving most of the specific protein-DNA and protein-protein interface interactions (data not shown). As an example, Figures 5B and 5C show the modeling of protein-protein interfaces for Oct-4 homodimers formed on the MORE and PORE (compare to Figures 2C and 2D). Like Ile159 of Oct-1, Ser159 in Oct-4 can play a pivotal role in the MORE interface: it could be involved in H bond formation with Gln6 from the other Oct-4 POU domain. The modeling, along with previous biochemical data (Botquin et al., 1998; Tomilin et al., 2000), suggests that the observed interface swapping is a property widely shared in the POU family. Clearly, the transcriptional properties of each POU factor and its regulatory mechanisms need to be better characterized so as to discover to what extent the potential of interface-domain swapping is generally used to acquire differential transcriptional activity.

Phosphorylation as a Regulator of Dimerization

The activities of Oct-1 and Pit-1 are modified in vitro as well as in vivo by phosphorylation of Ser107 or Thr107 from the POU_H domains of Oct-1 and Pit-1, respectively (Segil et al., 1991; Kapiloff et al., 1991). Phosphorylation also modifies the activities of Oct-2 (Pevzner et al., 2000) and the embryonic stem cell-specific transcription factor Oct-4 in vivo (Brehm et al., 1997), but their sites have not been mapped so far. The sequence alignment (Figure 5A) shows that position 159 in the Oct-4 POU domain is occupied by a serine as opposed to an isoleucine in Oct-1. In Oct-4, both serines at positions 107 and 159 are situated in a KR(**T/S**)**S**IE motif, which is a potential target site for phosphorylation by cAMP- or cGMP-dependent protein kinase. The first site (Ser107) is within the PORE POU_S-POU_H interface, and the second (Ser159) is within the MORE POU_S-POU_H interface. This is illustrated in the modeled POU_S-POU_H interfaces of Oct-4 in the MORE and PORE arrangements (Figures 5B and 5C). The Ser159Glu mutation, which mimics phosphorylation of Ser159 by a cellular protein kinase, selectively abolishes the MORE-type but not the PORE-type dimer formation (Figure 5D). In contrast, phosphor-

Table 1. Crystallographic Data Collection, Structure Solution, and Refinement

Crystal [Space Group]	λ (Å)	d(mi) (Å)	No. Data	Completeness (%)	Multiplicity	I/σ (Last Shell)	R_{sym}[a] (%)	Phasing Power[b] iso/ano	R_{cullis}[c] iso/ano
X-Ray Data Collection									
POU:MORE [C2]	0.8424	1.90	19950	95.3	4.6	24.4 (6.2)	3.9 (11.1)	—	—
POU:PORE [P6222]	0.8424	2.70	16717	99.5	5.9	23.0 (3.5)	5.8 (38.9)	—	—
POU:PORE(br1)-peak	0.9185	2.85	14471	99.8	10.4	17.4 (6.1)	10.6 (41.7)	4.94/0.90	0.26/0.95
POU:PORE(br1)-infl.	0.9190	2.85	14436	99.7	5.6	11.8 (5.6)	8.3 (31.0)	5.90/0.67	0.30/0.98
POU:PORE(br1)-remote	0.8856	2.85	14376	99.5	4.9	14.5 (5.2)	8.0 (24.2)	—/0.93	—/0.95

Crystal	Protein Atoms	DNA Atoms	Solvent Atoms	rmsd Bond Length (Å)	rmsd Bond Angles (°)	R_{cryst}[d] (%)	R_{free}[d] (%)	<B> (Å^2) Protein/DNA
Structure Refinement								
POU:MORE	1052	445	138	0.013	1.5	22.0	24.2	49/43
POU:PORE	2006	896	119	0.011	1.4	23.9	29.4	61/45

[a] $R_{sym} = \Sigma_{hkl}\Sigma_i|I_i(hkl) - <I(hkl)>|/\Sigma_{hkl}\Sigma_i I_i(hkl)$.
[b] Phasing power is defined as the ratio of the rms value of the heavy atom structure factor amplitudes and the rms value of the lack-of-closure error.
[c] R_{cullis} is the mean lack-of-closure error divided by the isomorphous/anomalous difference.
[d] R_{cryst} and $R_{free} = |\Sigma F_{obs} - F_{calc}|/\Sigma F_{obs}$; R_{free} is calculated with 5% of the data that were not used for refinement.

ylation of Ser107, which is imitated by Ser107Glu mutation, generally abolishes DNA binding of recombinant expressed Oct-1 and Oct-4 POU domains (data not shown). Our structures suggest that phosphorylation of Ser107, which faces the DNA backbone, leads to a steric clash in the POU_H-DNA interface that is sufficient to abolish formation of both MORE and PORE complexes. These data indicate that differential tissue- and cell cycle-specific phosphorylation could be an additional mechanism to specifically regulate POU dimer function in vivo.

Differential Recruitment by POU Dimers: A General Model

The functional properties of a wide range of transcription factors are altered by conformational changes induced by activators, repressors, and specific receptor ligands (Lefstin and Yamamoto, 1998). At the structural level, these changes often lead to the formation of additional helices, reorientation of loops, and rearrangements of hydrophobic cores. In contrast, members of the POU family lack structural flexibility within their POU subdomains. Nevertheless, they have evolved a specific regulatory mechanism that relies mainly on the flexible positioning of their subdomains, directed by the architecture and overall length of targeted DNA sequences. These DNA response elements not only induce either monomer or dimer binding of POU factors but also mediate the assembly of different quaternary arrangements stabilized by specific protein-protein interactions (see Figure 4). The distinct dimeric arrangements allow differential recruitment of cofactors, which exert diverse effects on transcription.

Figure 6 schematically outlines such a mechanism. It is only a certain configuration of POU dimers that provides protein surfaces accessible for interaction with a cofactor. In our example, the OBF-1 coactivator utilizes the accessible Oct-1 POU subdomain surfaces in the PORE-type configuration that are inaccessible in the MORE-type configuration (Figures 6A and 6B). Therefore, the MORE-type configuration fails to recruit OBF-1 (Tomilin et al., 2000). However, an opposite situation, in which the POU Oct-1 dimer formed on the MORE mediates the recruitment of a yet unknown specific cofactor, is also conceivable ("Y," Figure 6B). Furthermore, differences within the same POU dimer configuration, generated by different spacing arrangements of half-sites, may also lead to selective cofactor recruitment, as recently demonstrated for the pituitary-specific POU factor Pit-1 (Scully et al., 2000). Two structures of Pit-1 bound to two related DNA response elements within the *prolactin* (*Prl*) and the *growth hormone* (*GH*) promoters show how the same dimer arrangement can accommodate different spacing between the POU subdomain binding sites (Scully et al., 2000). These two promoter motifs are almost identical, apart from the insertion of additional TT nucleotides between the two half-sites in the *GH* element. The extended conformation adopted by Pit-1 on *GH* enables recruitment of a corepressor complex containing N-CoR, leading to repression of *GH* transcription in lactotrope pituitary tissues. However, the molecular basis for differential recruitment of N-CoR still needs to be determined. Other POU proteins, such as Oct-1, Oct-2, Oct-4, and Oct-6, are also capable of preserving dimerization if the half-site spacing changes in the same MORE-type arrangement (Tomilin et al., 2000). Thus, these POU factors may be regulated via a similar mechanism (Figures 6B and 6C).

To understand the biological function of each dimer type, it will be necessary to selectively mutate one or the other interface in cellular and animal model systems. The identification of dimer-specific cofactors will be important to further our understanding of the biological processes regulated by POU proteins. Of special interest are dimer-specific cofactors for POU proteins that are components of the development of immune response (Oct-1) and maintenance of stem cell pluripotency and germ cell lineage (Oct-4).

Conclusion

The two structures of the Oct-1 POU factor in complex with the MORE and PORE DNA motifs reveal two alterna-

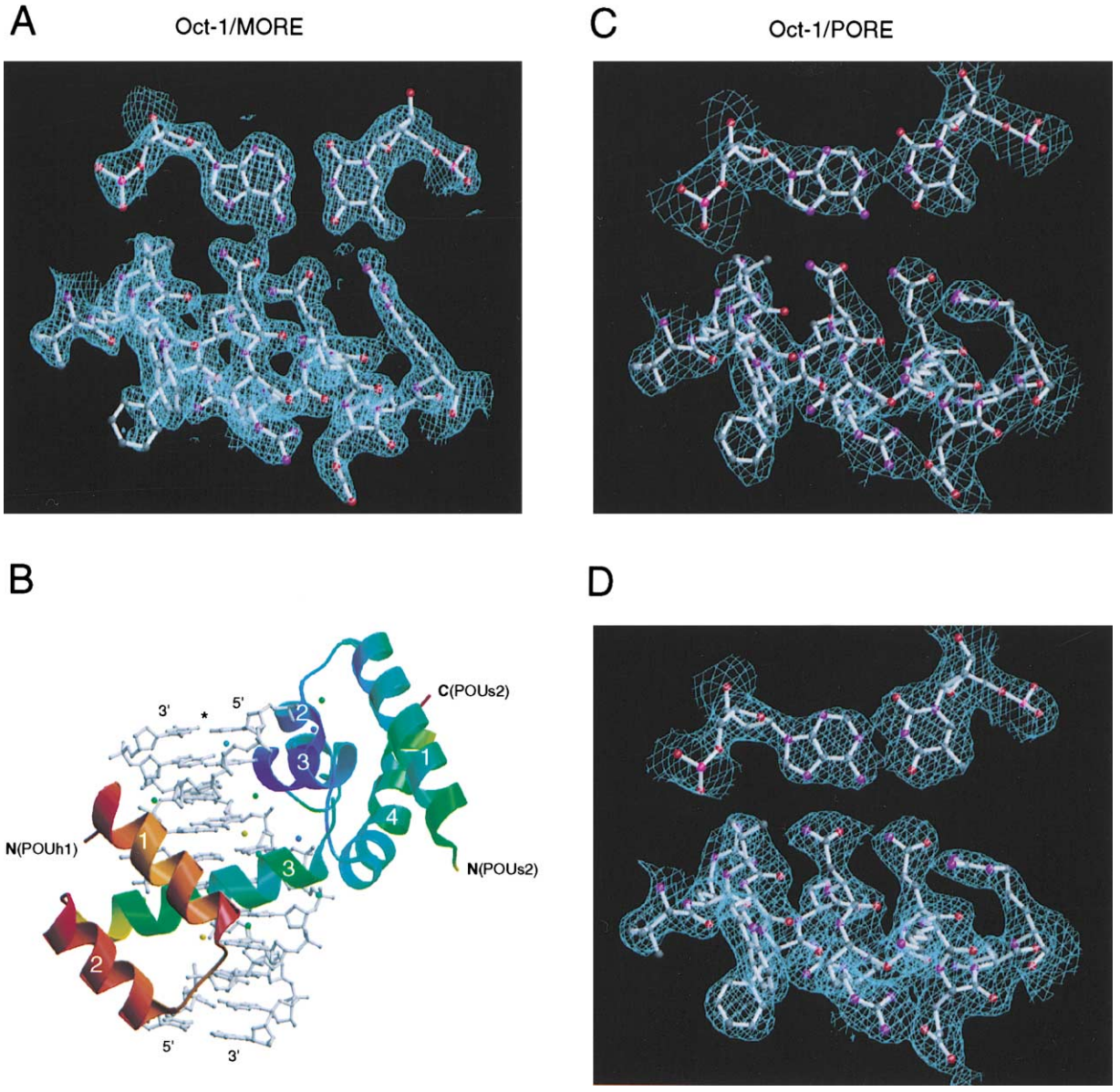

Figure 7. Crystallographic Structure Determination of the Oct-1/MORE and Oct-1/PORE Complexes

(A) Oct-1/MORE: electron density from σ_A-weighted, simulated annealed, 2Fo − Fc omit map (1.9 Å) calculated with the final model—but omitting all atoms depicted on the figure.

(B) Crystal structure of the Oct-1/MORE half dimer. The full dimer is generated by application of a crystallographic 2-fold axis indicated by the asterisk. The content of the asymmetric unit is colored according to the averaged local displacement factors, ranging from blue (20 Å^2) to red (75 Å^2). All water molecules within the protein-DNA interface are shown as small spheres colored by their refined atomic temperature factors.

(C) Oct-1/PORE: experimental electron density map (2.85 Å) calculated after solvent flattening.

(D) Oct-1/PORE: electron density from σ_A-weighted simulated annealed 2Fo − Fc omit map (2.7 Å) calculated with the final model. The figures show the Val146-Arg158 helical region of both complexes with an AT base pair. Asn151 contacts the adenine base by two H bonds in the middle of the figures.

tive and unrelated dimer arrangements of the same polypeptide chain. They provide direct evidence for the unique property of POU transcription factors to regulate their functional properties by forming different dimer assemblies. Previously, protein-protein interface swapping has been observed in a number of proteins with a potential for monomer/dimer transitions leading in some cases to pathological effects (Schlunegger et al., 1997). The members of the POU transcription factor family could serve as a paradigm to regulate protein function by protein-protein interface swapping.

Experimental Procedures

Protein Expression, Purification, and Crystallization

Protein expression and purification, as well as details of the crystallization procedure, are described elsewhere (Reményi et al., 2001).

The crystallization trials for the Oct-1/PORE complex were carried out with chemically synthesized oligonucleotides containing a modified PORE motif (ATTTGAAAGGCAAAT, T→G) that enhanced homogenous dimer formation, showing comparable functional properties to the original PORE motif (Botquin et al., 1998). The Oct-1/MORE complex crystals were grown with a 21 bp oligonucleotide with TA-overhangs from 22%–24% [v/w] PEG3350, 50 mM HEPES (pH 7.0), and 1.8 mM spermine, at 20°C. The Oct-1/MORE crystals belong to the space group C2 with unit cell dimensions a = 93.3 Å, b = 52.4 Å, c = 69.0 Å, and β = 127.6°. The Oct-1/PORE cocrystals with a blunt-end 22 bp oligonucleotide grew from 20%–23% [v/w] PEG1000, 100 mM Na-citrate (pH 5.3), and 5% [v/v] glycerol. The Oct-1/PORE complex crystallized in space group P6(2)22 with unit cell dimensions a = b = 131.2 Å, c = 116.8 Å.

Data Collection, Structure Solution, and Refinement

Crystallographic Data Collection

Crystals were mounted on nylon loops and flash-frozen in liquid nitrogen prior to data collection at 100 K. The native datasets were collected on the wiggler beam line BW7B at EMBL/DESY, Hamburg, at a fixed wavelength of 0.8424 Å, using a Mar 345 mm Imaging Plate. The MAD dataset of Oct-1/PORE complex was collected at beam line BW7A at EMBL/DESY, Hamburg, at three different wavelengths. The data were recorded with a Mar 165 mm-CCD detector. Raw data were reduced and scaled with the HKL suite (Otwinowski and Minor, 1997). Details of the crystallographic data collection are given in Table 1.

Structure Solution of the Oct-1/MORE Complex

The structure of the Oct-1/MORE complex was solved by molecular replacement with the AMoRe software (Navaza, 1994). The search model consisted of a protein-DNA complex comprising the POU_S domain and the ATGC half of the octamer binding site (Klemm et al., 1994). The semiautomatic density interpretation program BLOB (Diller et al., 1999) was used for DNA model building. After having identified a continuous double spiral along the c-axis in the unit cell, the base pairs were modified according to the sequence used for crystallization. The "WarpNtrace" procedure, implemented in ARP 5.1 (Perrakis et al., 1999) with all data to 1.9 Å, was used to extend the model, to position the side chains of the POU_S, and to trace the recognition helix 3 of the POU_H domain. The model was completed by iterative cycles of refinement interspersed with σ_A-weighted Fo − Fc map calculations in CNS (Brunger et al., 1998) and manual model additions in O version 6.2 (Jones et al., 1991). The protein binds to the DNA as a symmetrical homodimer, with the symmetry axis of this complex located on the crystallographic 2-fold axis perpendicular to the pseudopalindromic center of each MORE oligonucleotide (upper strand, 5′-TCCTCATGCAT*ATGC ATCTCC-3′; lower strand, 5′-AGGGAGATGCAT*ATGCATGAGG-3′). The complete protein-DNA dimer complex was generated by the crystallographic 2-fold axis. In the structure determination and refinement, the two halves of the MORE sequence were treated identically. The final model consists of 75 residues of the POU_S domain (1–75) and 56 residues of the POU_H domain (104–160) bound to an 11 bp oligonucleotide containing the half-site of the MORE motif (ATGCAT) (Figure 7B).

Structure Solution of the Oct-1/PORE Complex

The structure of the Oct-1/PORE complex was solved by the MAD method, using a bromine derivative in which the thymine bases were replaced by 5-bromo-uracils. Thus, this derivative contained two bromo-uracils ("U") on the upper (5′-CACATTUGAAAGGCAAAUG GAG-3′) and two on the lower strand (5′-CTCCATTUGCCTTT CAAAUGTG-3′). The heavy atom sites were identified using SHEL-X (Sheldrick, 1998). Heavy atom position refinement and phase calculation were carried out in SHARP (La Fortelle and Bricogne, 1997), using all X-ray data between 20.0–2.85 Å resolution. The initial phases were further improved by solvent flattening with SOLOMON (CCP4, 1994). An electron density map extending to 2.85 Å and calculated with the solvent-flattened phases was used for map interpretation. The model was built and completed as described for the Oct-1/MORE complex (see above).

The asymmetric unit contains an Oct-1 dimer bound to the PORE motif (ATTTGAAAGGCAAAT). The final model consists of 2 × 70 residues of the POU_S domain (6–75) and 2 × 57 residues of the POU_H domain (102–159) complexed with a 22 bp oligonucleotide. The linker region (76–102) connecting the two subdomains could not be located in the electron density map for either complex.

Structure Refinement

Structure refinement and map calculations, using all the data from 20 Å to 1.9 Å for the Oct-1/MORE and from 20 Å to 2.7 Å for the Oct-1/ PORE complex, respectively, were carried out with the software package CNS (Brunger et al., 1998). The final Oct-1/MORE model has an R factor of 22.0% and R_{free} of 24.2%, while the final Oct-1/PORE model has an R factor of 23.9% and R_{free} of 29.4%. None of the residues are located in the disallowed region on the Ramachandran plot. 96% of the residues are in the most-favored region of the Oct-1/MORE and 91% are in the most-favored region of the Oct-1/PORE complex (PROCHECK, Laskowski et al., 1993). Further details of the structure refinement are given in Table 1. Figures 7A and 7D display the electron density of the recognition helix (helix 3) from POU_H with an AT base pair from the σ_A-weighted, simulated annealed 2Fo − Fc omit map calculated with the final model of the Oct-1/MORE and the Oct-1/PORE complex, respectively. The quality of the phases after solvent flattening for the Oct-1/PORE MAD phasing experiment is illustrated in Figure 7C. The figures were prepared using MOLSCRIPT, Raster3D, BOBSCRIPT, and DINO (http://www.dino3d.org).

Site-Directed Mutagenesis and Electrophoretic Mobility Shift Assay (EMSA)

A pET24d (Novagen)-based vector containing the wild-type sequence of the Oct-1 DNA binding segment was used as a template for the Transformer Site-Directed Mutagenesis Kit (Clontech). The proteins were expressed with histidine tags in *E. coli* at 30°C and purified from the soluble fraction on Ni-NTA agarose (Qiagen). The wild-type full-length and the S159E mutant Oct-4 protein were expressed similarly, but the protein was found in the insoluble fraction. The resolubilized material (in 6 M GuHCl) was loaded onto a Ni-NTA agarose affinity column, washed, refolded by quick removal of the denaturant, and finally eluted from the column. The full-length OBF-1 protein was expressed and purified similar to the POU domain of Oct-1 (Reményi et al., 2001). ΔOBF-1 used in the EMSA in Figure 3 was chemically synthesized and is identical to the 44 amino acid-containing peptide used for crystallization by Chasman et al. (1999).

The bacterially expressed mutants and the wild-type proteins were tested in EMSAs as described in Sylvester and Schöler (1994) with the following radioactively labeled oligonucleotides: Igκ, 5′-ctg actcctgccttcagggtATGCAAATtattaagtctcgag-3′; MORE, 5′-ctgaaagt taaaatctcATGCATATGCATggaaaagcaag-3′; and PORE, 5′-ctgaaagt taaaatcacATTTGAAAGGCAAATggaaaagcaag-3′.

Acknowledgments

We thank Christoph Müller for critical comments on and Areti Malapetsa for critically reading the manuscript. The work in Hamburg was supported by the EMBL (M.W.). The work at the University of Pennsylvania was supported by the Marion Dilley and David George Jones Funds and the Commonwealth and General Assembly of Pennsylvania (H.R.S.).

Received May 17, 2001; revised August 2, 2001.

References

Botquin, V., Hess, H., Fuhrmann, G., Anastassiadis, C., Gross, M.K., Vriend, G., and Schöler, H.R. (1998). New POU dimer configuration mediates antagonistic control of an osteopontin preimplantation enhancer by Oct-4 and Sox-2. Genes Dev. *12*, 2073–2090.

Brehm, A., Ohbo, K., and Schöler, H. (1997). The carboxy-terminal transactivation domain of Oct-4 acquires cell specificity through the POU domain. Mol. Cell. Biol. *17*, 154–162.

Brunger, A.T., Adams, P.D., Clore, G.M., DeLano, W.L., Gros, P., Grosse-Kunstleve, R.W., Jiang, J.S., Kuszewski, J., Nilges, M., Pannu, N.S., et al. (1998). Crystallography & NMR system: a new software suite for macromolecular structure determination. Acta Crystallogr. D. Biol. Crystallogr. *54*, 905–921.

CCP4 (Collaborative Computational Project 4) (1994). The CCP4

suite: programs for protein crystallography. Acta Crystallogr. D. *50*, 760–763.

Chasman, D., Cepek, K., Sharp, P.A., and Pabo, C.O. (1999). Crystal structure of an OCA-B peptide bound to an Oct-1 POU domain/octamer DNA complex: specific recognition of a protein-DNA interface. Genes Dev. *13*, 2650–2657.

Diller, D.J., Pohl, E., Redinbo, M.R., Hovey, B.T., and Hol, W.G. (1999). A rapid method for positioning small flexible molecules, nucleic acids, and large protein fragments in experimental electron density maps. Proteins *36*, 512–525.

Herr, W., and Cleary, M.A. (1995). The POU domain: versatility in transcriptional regulation by a flexible two-in-one DNA-binding domain. Genes Dev. *9*, 1679–1693.

Jacobson, E.M., Li, P., Rosenfeld, M.G., and Aggarwal, A.K. (1996). Crystallization and preliminary X-ray analysis of Pit-1 POU domain complexed to a 28 base pair DNA element. Proteins *24*, 263–265.

Jacobson, E.M., Li, P., Leon-del-Rio, A., Rosenfeld, M.G., and Aggarwal, A.K. (1997). Structure of Pit-1 POU domain bound to DNA as a dimer: unexpected arrangement and flexibility. Genes Dev. *11*, 198–212.

Jones, T.A., Zou, J.Y., Cowan, S.W., and Kjeldgaard (1991). Improved methods for binding protein models in electron density maps and the location of errors in these models. Acta Crystallogr. A. *47*, 110–119.

Kapiloff, M.S., Farkash, Y., Wegner, M., and Rosenfeld, M.G. (1991). Variable effects of phosphorylation of Pit-1 dictated by the DNA response elements. Science *253*, 786–789.

Klemm, J.D., Rould, M.A., Aurora, R., Herr, W., and Pabo, C.O. (1994). Crystal structure of the Oct-1 POU domain bound to an octamer site: DNA recognition with tethered DNA-binding modules. Cell *77*, 21–32.

La Fortelle, E., and Bricogne, G. (1997). Maximum-likelihood heavy-atom parameter refinement in the MIR and MAD method. In Methods Enzymol., Macromolecular Crystallography. R.M. Sweet and C.W.J. Carter, eds. (New York: Academic Press), pp. 472–494.

Laskowski, R.A., MacArthur, M.W., Moss, D.S., and Thornton, J.M. (1993). PROCHECK: a program to check the stereochemical quality of protein structures. J. Appl. Crystallogr. *26*, 283–291.

Lavery, R., and Sklenar, H. (1988). The definition of generalized helicoidal parameters and of axis curvature for irregular nucleic acids. J. Biomol. Struct. Dyn. *6*, 63–91.

Lee, B.L., and Richards, F.M. (1971). The interpretation of protein structures: estimation of static accessibility. J. Mol. Biol. *55*, 379–400.

Lefstin, J.A., and Yamamoto, K.R. (1998). Allosteric effects of DNA on transcriptional regulators. Nature *392*, 885–888.

Luscombe, N.M., Laskowski, R.A., and Thornton, J.M. (1997). NUCPLOT: a program to generate schematic diagrams of protein-nucleic acid interactions. Nucleic Acids Res. *25*, 4940–4945.

Mangelsdorf, D.J., and Evans, R.M. (1995). The RXR heterodimers and orphan receptors. Cell *83*, 841–850.

Navaza, J. (1994). AMoRe: an automated package for molecular replacement. Acta Crystallogr. A. *50*, 157–163.

Otwinowski, Z., and Minor, W. (1997). Processing of x-ray diffraction data collected in oscillation mode. Methods Enzymol. *A276*, 307–325.

Perrakis, A., Morris, R., and Lamzin, V.S. (1999). Automated protein model building combined with iterative structure refinement. Nat. Struct. Biol. *6*, 458–463.

Pevzner, V., Kraft, R., Kostka, S., and Lipp, M. (2000). Phosphorylation of Oct-2 at sites located in the POU domain induces differential down-regulation of Oct-2 DNA-binding ability. Biochem. J. *347*, 29–35.

Phillips, K., and Luisi, B. (2000). The virtuoso of versatility: POU proteins that flex to fit. J. Mol. Biol. *302*, 1023–1039.

Rhee, J.M., Gruber, C.A., Brodie, T.B., Trieu, M., and Turner, E.E. (1998). Highly cooperative homodimerization is a conserved property of neural POU proteins. J. Biol. Chem. *273*, 34196–34205.

Reményi, A., Pohl, E., Schöler, H.S., and Wilmanns, M. (2001). Crystallization of redox-insensitive Oct1 POU domain with different DNA response elements. Acta Crystallogr. D., in press.

Ryan, A.K., and Rosenfeld, M.G. (1997). POU domain family values: flexibility, partnerships, and developmental codes. Genes Dev. *11*, 1207–1225.

Sauter, P., and Matthias, P. (1998). Coactivator OBF-1 makes selective contacts with both the POU-specific domain and the POU homeodomain and acts as a molecular clamp on DNA. Mol. Cell. Biol. *18*, 7397–7409.

Schlunegger, M.P., Bennett, M.J., and Eisenberg, D. (1997). Oligomer formation by 3D domain swapping: a model for protein assembly and misassembly. Adv. Prot. Chem. *50*, 61–122.

Schöler, H.R. (1991). Octamania: the POU factors in murine development. Trends Genet. *7*, 323–329.

Schöler, H.R., Hatzopoulos, A.K., Balling, R., Suzuki, N., and Gruss, P. (1989). A family of octamer-specific proteins present during mouse embryogenesis: evidence for germline-specific expression of an Oct factor. EMBO J. *8*, 2543–2550.

Scully, K.M., Jacobson, E.M., Jepsen, K., Lunyak, V., Viadiu, H., Carriere, C., Rose, D.W., Hooshmand, F., Aggarwal, A.K., and Rosenfeld, M.G. (2000). Allosteric effects of Pit-1 DNA sites on long-term repression in cell type specification. Science *290*, 1127–1131.

Segil, N., Roberts, S.B., and Heintz, N. (1991). Mitotic phosphorylation of the Oct-1 homeodomain and regulation of Oct-1 DNA binding activity. Science *254*, 1814–1816.

Sheldrick, G.M. (1998). SHELX: application to macromolecules. In Direct Methods for Solving Macromolecular Structures, S. Fortier, ed. (Dordrecht: Kluwer Academic Publishers), pp. 401–411.

Staudt, L.M., Singh, H., Sen, R., Wirth, T., Sharp, P.A., and Baltimore, D. (1986). A lymphoid-specific protein binding to the octamer motif of immunoglobulin genes. Nature *323*, 640–643.

Sylvester, I., and Schöler, H.R. (1994). Regulation of the Oct-4 gene by nuclear receptors. Nucleic Acids Res. *22*, 901–911.

Tomilin, A., Reményi, A., Lins, K., Bak, H., Leidel, S., Vriend, G., Wilmanns, M., and Schöler, H.R. (2000). Synergism with the coactivator OBF-1 (OCA-B, BOB-1) is mediated by a specific POU dimer configuration. Cell *103*, 853–864.

Venter, J.C., et al. (2001). The sequence of the human genome. Science *291*, 1304–1350.

Vriend, G. (1990). WHAT IF: a molecular modeling and drug design program. J. Mol. Graph. *8*, 52–56.

Accession Numbers

Coordinates of the Oct-1/MORE and the Oct-1/PORE complex have been deposited into the Protein Data Bank with the ID codes 1e3o and 1hf0, respectively.